

Subject: Detailed Responses to Reviewers: Liu, H., Maghoul, P., and Shalaby, A.: Seismic physics-based characterization of permafrost sites using surface waves, *The Cryosphere Discuss.* [preprint], <https://doi.org/10.5194/tc-2021-219>, in review, 2021.

Date: November 15, 2021

The authors are grateful for the valuable comments and kind consideration of our submission. Detailed responses and revisions based on these comments are listed below.

1 General Comments

This article proposes an original use of seismic methods to characterize a permafrost area. The main interest of the study lies in the identification and interpretation of two types of Rayleigh waves propagating in a frozen porous medium. The separate inversion of the two dispersion curves provides a hybrid method for determining independently the physical and mechanical properties of the medium, thanks to the difference in the respective sensitivity of these two waves to these properties. The article invites the use of this method to characterize a permafrost medium, as it appears to be more efficient and requires fewer a priori assumptions about the investigated medium.

The authors mention various applications to the detection and characterization of permafrost, ranging from civil engineering and infrastructure monitoring to the assessment of the potential vulnerability of certain areas to permafrost degradation and associated feedbacks.

The article is well structured and adequately written. A significant contribution is that authors used seismic data collected at a site in Svalbard, and applied their processing to this experiment, to show a real application of their method.

In my opinion the paper deserves publication after minor revisions.

1. First, the contribution of this study to the current knowledge of seismic waves propagating in permafrost is not very comprehensible to the reader. The lack of references about the poroelastic model and the lack of physical interpretation of the two Rayleigh waves should be corrected.

From a poromechanical point of view, permafrost (frozen soil) is a multi-phase porous medium that is composed of a solid skeletal frame and pores filled with water and ice with different proportions. Three types of P wave (P1, P2 and P3) and two types of S wave (S1, S2) coexist in three-phase frozen porous media (Carcione et al., 2000; Carcione and Seriani, 2001; Carcione et al., 2003). The P1 and S1 waves are the longitudinal and transverse waves propagating in the solid skeletal frame, respectively, but are also dependent on the interactions with pore ice and pore water (Carcione and Seriani, 2001). The P2 and S2 waves propagate mainly within pore ice (Leclaire et al., 1994). Similarly, the P3 wave is due to the interaction between the pore water and the solid skeletal frame. However, the understanding of surface wave propagation in permafrost is still limited in the literature. The current surface wave analysis in foundation permafrost does

not consider the interaction of different wave modes (P1, P2, P3, S1 and S2) due to the multiphase poroelastic properties of permafrost at the near surface and still assume permafrost soils as a solid elastic material (Leblanc et al., 2006; 2017; Krautblatter et al., 2014, Dou et al., 2014; Ajo-Franklin et al.). In this paper, we have identified and demonstrated the formation of two types of Rayleigh waves (R1 and R2) at the surface in permafrost sites due to the interaction of different phases (e.g., solid skeletal frame, pore-water and pore-ice). More importantly, we concluded that the phase velocity of the R1 wave is mostly sensitive to the shear modulus of the solid skeletal frame; it is also dependent on the bulk modulus, porosity, and degree of saturation of ice. On the other hand, the phase velocity of the R2 wave is almost independent of the mechanical properties of the solid skeletal frame, while it is strongly affected by the porosity and degree of saturation of ice, as shown in Figure 1e and 1f.

References about the three-phase poroelastic model used in this paper have been added to the manuscript (Leclaire et al., 1994 and Carcione et al., 2000).

To physically interpret the two Rayleigh waves, a uniform frozen soil layer is used to show the propagation of different types of P and S waves and subsequently the formation of Rayleigh waves (R1 and R2) at the surface. It is assumed that an impulse load with a dominant frequency of 100 Hz is applied at the ground surface. The wave propagation analysis was performed in clayey soils by assuming a porosity (n) of 0.5, a degree of saturation of unfrozen water (S_r) of 50%, a bulk modulus (K) of 20.9 GPa and a shear modulus (G) of 6.85 GPa for the solid skeletal frame (helgerud et al., 1999). The velocities of the P1 and P2 waves are calculated as 2,628 m/s and 910 m/s, respectively, based on the relations given in Appendix A in the manuscript. The velocity of P3 wave (16 m/s) is relatively insignificant in comparison to P1 and P2 wave velocities. Similarly, the velocities of the S1 and S2 waves are calculated as 1,217 m/s and 481 m/s, respectively. Accordingly, the observed displacements measured at the ground surface with an offset from the impulse load ranging from 0 to 120 m are illustrated in Figure 1a. Figure 1b to illustrate the waveforms of R1 and R2 waves at the offset of 80 m. Figure 1c and 1d illustrate the appearance of two types of Rayleigh waves (R1 and R2) in a three-phase permafrost subsurface at 70 ms and 100 ms, respectively. We found the velocity of R1 and R2 is 1,150 m/s and 450 m/s using the three-phase dispersion relation derived in this paper. It is commonly known that the Rayleigh wave is slightly slower than the shear wave velocity and the ratio of Rayleigh wave and shear wave velocity ranges from 0.92-0.95 for Poisson's ratio greater than 0.3 (Kazemirad et al., 2013). From this analysis, we found the ratio of R1 and S1 wave velocity is around 0.93. Similarly, the ratio of R2 and S2 wave velocity is around 0.94. Therefore, we can conclude that R1 waves appear due to the interaction of P1 and S1 waves since the phase velocity of R1 waves is slightly slower than the phase velocity of S1 waves. Similarly, R2 waves appear due to the interaction of P2 and S2 waves since the phase velocity of R2 waves is also slightly slower than the phase velocity of S2 waves.

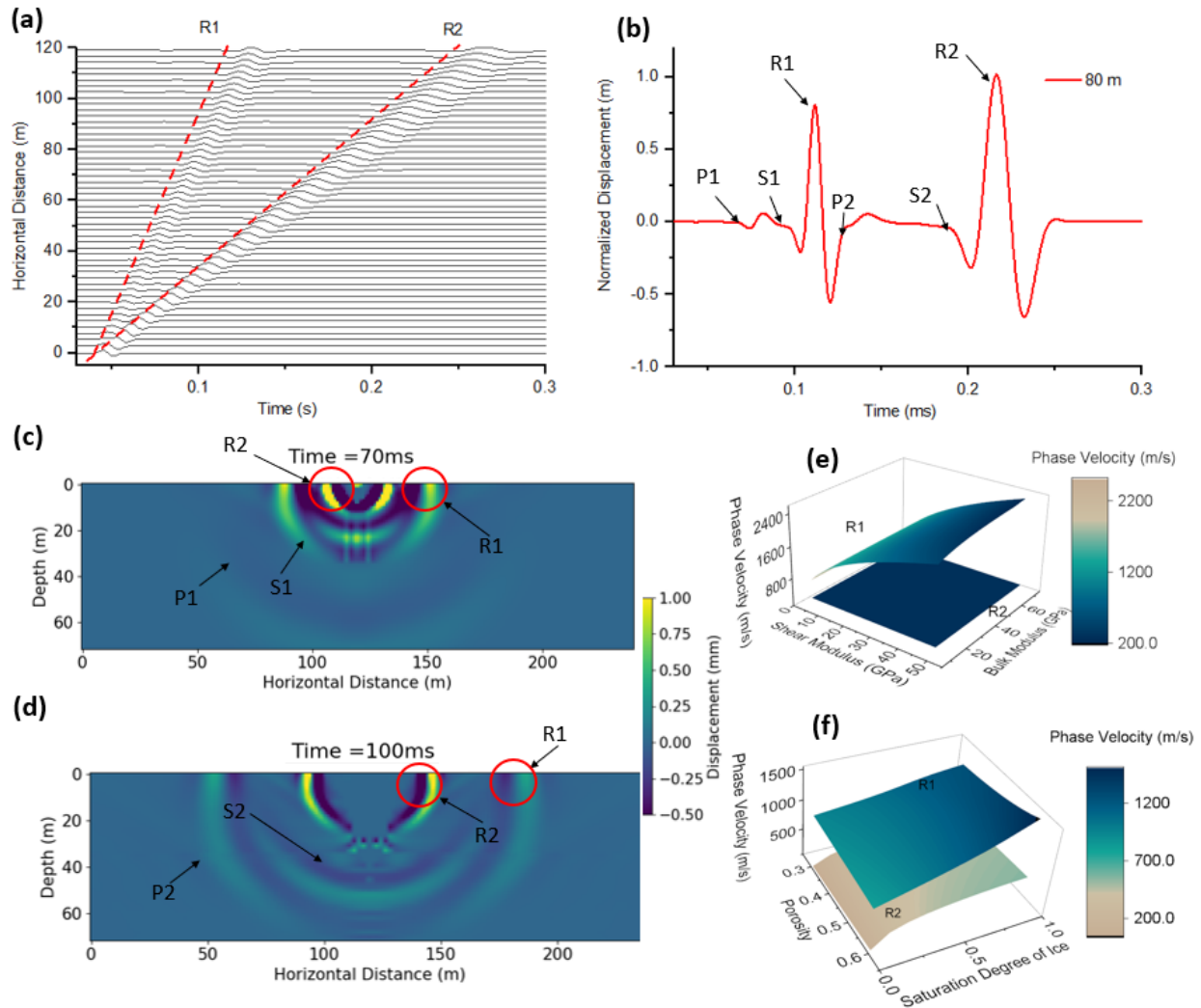


Figure 1: **(a)** Theoretical time-series measurements for R1 and R2 Rayleigh waves at the ground surface **(b)** Waveforms of R1, R2 and other wave modes at the offset of 80 m. **(c)** Displacement contour at time 70 ms. **(d)** Displacement contour at time 100 ms with the labeled R1 and R2 Rayleigh waves. **(e)** Effect of shear modulus and bulk modulus of the solid skeletal frame on phase velocity of R1 and R2 waves. **(f)** Effect of degree of saturation of ice on the phase velocity of R1 and R2 waves.

Reference:

Ajo-Franklin, J., Dou, S., Daley, T., Freifeld, B., Robertson, M., Ulrich, C., & Wagner, A. (2017). Time-lapse surface wave monitoring of permafrost thaw using distributed acoustic sensing and a permanent automated seismic source. In SEG Technical Program Expanded Abstracts 2017 (pp. 5223-5227). Society of Exploration Geophysicists.

Leblanc, A. M., Fortier, R., Cosma, C., & Allard, M. (2006). Tomographic imaging of permafrost using three-component seismic cone-penetration test. *Geophysics*, 71(5), H55-H65.

Krautblatter, M., & Draebing, D. (2014). Pseudo 3-D P wave refraction seismic monitoring of permafrost in steep unstable bedrock. *Journal of Geophysical Research: Earth Surface*, 119(2), 287-299.

Dou, S., & Ajo-Franklin, J. B. (2014). Full-wavefield inversion of surface waves for mapping embedded low-velocity zones in permafrost. *Geophysics*, 79(6), EN107-EN124.

Carcione, J. M., & Seriani, G. (2001). Wave simulation in frozen porous media. *Journal of Computational Physics*, 170(2), 676-695.

Carcione, J. M., Gurevich, B., & Cavallini, F. (2000). A generalized Biot–Gassmann model for the acoustic properties of shaley sandstones1. *Geophysical Prospecting*, 48(3), 539-557.

Carcione, J. M., Santos, J. E., Ravazzoli, C. L., & Helle, H. B. (2003). Wave simulation in partially frozen porous media with fractal freezing conditions. *Journal of Applied Physics*, 94(12), 7839-7847.

Helgerud, M. B., Dvorkin, J., Nur, A., Sakai, A., & Collett, T. (1999). Elastic-wave velocity in marine sediments with gas hydrates: Effective medium modeling. *Geophysical Research Letters*, 26(13), 2021-2024.

Leclaire, P., Cohen-Ténoudji, F., & Aguirre-Puente, J. (1994). Extension of Biot's theory of wave propagation to frozen porous media. *The Journal of the Acoustical Society of America*, 96(6), 3753-3768.

Kazemirad, S., & Mongeau, L. (2013). Rayleigh wave propagation method for the characterization of a thin layer of biomaterials. *The Journal of the Acoustical Society of America*, 133(6), 4332-4342.

Horn, R. A. and Johnson, C. R.: *Matrix analysis*, Cambridge university press, 2012.

2. Also, the authors should include a fuller explanation of their field experiment in Svalbard (with a figure), to clarify what data they have collected and what their real contribution (instrumentation, data processing, ...) to this site.

This study mainly focuses on the development of a MASW signal processing technique for field investigation of permafrost sites using the decomposition of two Rayleigh waves. As indicated in the manuscript (line 184-187), the field experiment used in this study was performed by Glazer et al., (2020). Glazer et al., (2020) aimed to study the the effect of nearby glacial ice and surface water-courses on the formation of different ice-bearing sediments (development of permafrost) within the late Quaternary marine terraces. In this paper, the same experimental data collected by Glazer et al., 2020 is used to demonstrate the inversion analysis based on R1 and R2 Rayleigh waves that we presented in this paper. A summary of the field experiment and site description has been summarized in the manuscript as: 'The case study site is located at the Fuglebekken coastal area in SW Spitsbergen, Svalbard (77°00'30"N and 15°33'00"E). The study area has a a thick layer of unconsolidated sediments that are suitable for near-surface geophysical investigations (Glazer et al., 2020). The unconsolidated sedimentary rock contains a high proportion of pore spaces; consequently, they can accumulate a large volume of pore-water or pore-ice. It was reported by Szymański et al. (2013) that this study site also contains a lot of coarse sandy soils and gravels based on the direct sampling methods at the top 15 cm. The direct sampling results also confirmed that the study site

is very wet and the water table is very high (around 15 cm) (Szymański et al. 2013). From meteorological records, the mean annual air temperature (MAAT) at the testing site was historically below the freezing point, but more recently and due to a trend of climate warming, the MAAT recorded in 2016 is approaching 0°C (Glazer et al., 2020). Glazer et al., (2020) performed both seismic surveys (MASW test) and electrical resistivity investigations at the site in September 2017 to study the evolution and formation of permafrost considering surface watercourses and marine terrace. The MASW test was performed by using 60 geophone receivers with a frequency of 4.5 Hz spaced at regular 2 m intervals. In this case study, the same experimental data collected by Glazer et al., (2020) is used to demonstrate the inversion analysis based on R1 and R2 Rayleigh waves presented above. Figure 2a shows the location of the test site. Figure 2b, 2c and 2c show the test site with different soil types (silty, clayey and sandy sediment as well as gravels). Figure 2e illustrates the collected original seismic measurements at distances between 0 m and 120 m (hereafter referred to Section 1). The R1 and R2 Rayleigh waves are identified to obtain the experimental dispersion relations (Figure 2e and 2f). The phase velocity of R1 wave increases with frequency from 24 Hz to 80 Hz. The phase velocity of R2 wave decreases with frequency in the span of 18 Hz to 32 Hz. The largest wavelength is 22 m, calculated by the ratio of phase velocity of 404 m/s and a frequency of 18 Hz. The investigation depth in this study is focused on the first 11 m (based on the recommendation that MASW investigation depth is roughly half of the maximum wavelength (Olafsdottir et al., 2018)).

The main contribution of this study is that we proposed a hybrid inverse and multi-phase poromechanical approach for in-situ characterization of permafrost sites using the decomposition of two Rayleigh waves. In this method, we quantify the physical properties such as ice content, unfrozen water content, and porosity as well as the mechanical properties such as the shear modulus and bulk modulus of permafrost or soil layers. The MASW seismic investigation in the field site located at SW Spitsbergen, Svalbard is used to demonstrate the role of two different types of Rayleigh waves in characterizing the permafrost. Our results demonstrate the potential of seismic surface wave testing accompanied by our proposed hybrid inverse and poromechanical dispersion model for the assessment and quantitative characterization of permafrost sites. The highlights of this research include:

- Proposed a novel physics-based signal processing algorithm to quantitatively estimate the physical and mechanical properties of a permafrost site by surface waves
- Identified the existence of two types of Rayleigh waves (R1 and R2) where R1 travels relatively faster than R2 in a permafrost site
- The R1 wave velocity depends strongly on the soil type and mechanical properties (e.g., shear modulus and bulk modulus) of permafrost layers
- The R2 wave velocity is highly sensitive to the physical properties (e.g., unfrozen water content, ice content) of permafrost layers

Reference:

Glazer, M., Dobiński, W., Marciniak, A., Majdański, M., & Błaszczuk, M. (2020). Spatial distribution and controls of permafrost development in non-glacial Arctic catchment over the Holocene, Fuglebekken, SW Spitsbergen. *Geomorphology*, 358, 107128.

Szymański, W., Skiba, S., & Wojtuń, B. (2013). Distribution, genesis, and properties of Arctic soils: a case study from the Fuglebekken catchment, Spitsbergen. *Polish Polar Research*, 289-304.

Olafsdottir, E. A., Erlingsson, S., & Bessason, B. (2018). Tool for analysis of multichannel analysis of surface waves (MASW) field data and evaluation of shear wave velocity profiles of soils. *Canadian Geotechnical Journal*, 55(2), 217-233.

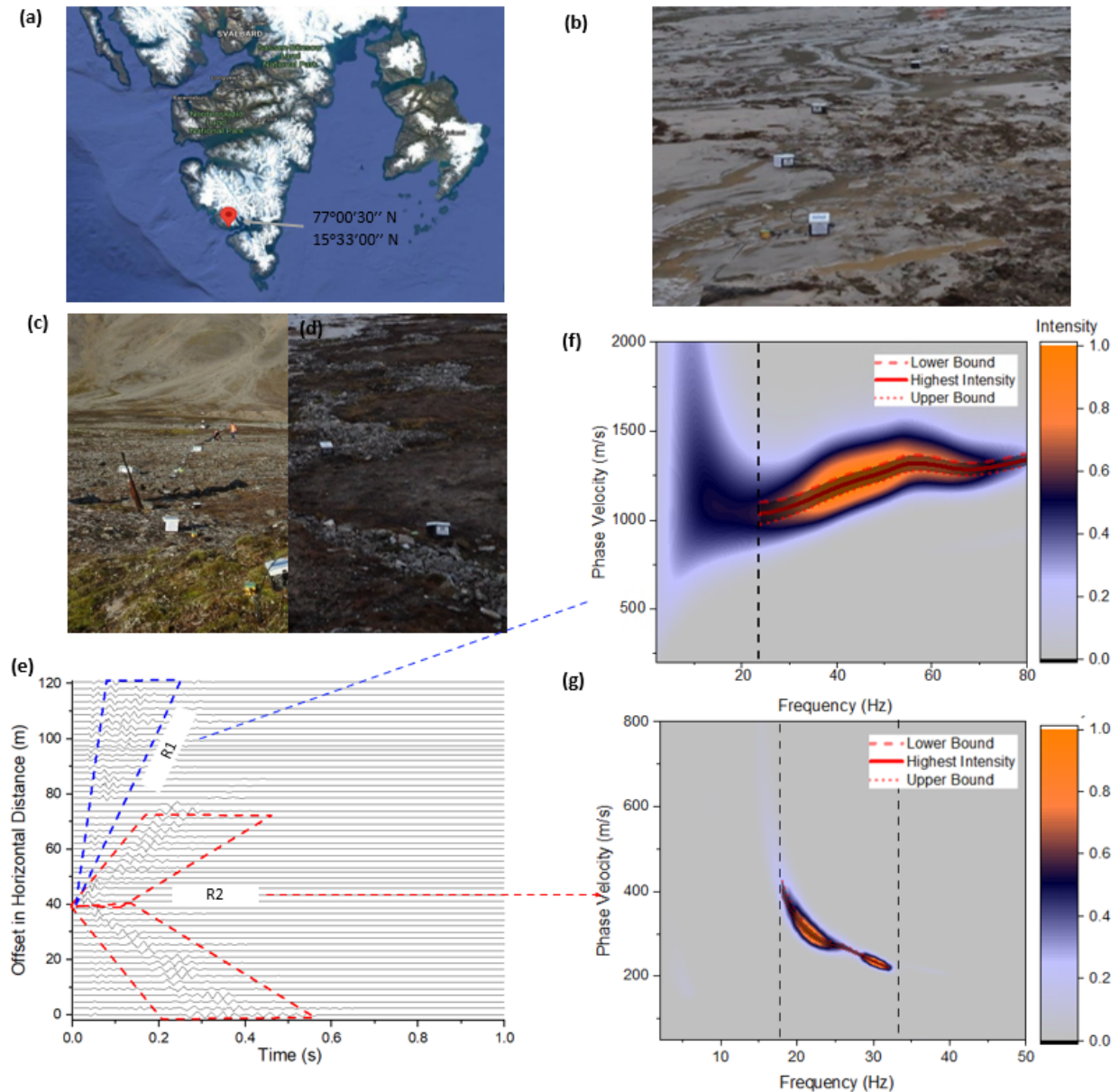


Figure 2: Surface wave measurement in Section 1 (from 0 m to 120 m). **(a)** Study area in Holocene, Fuglebekken, SW Spitsbergen. **(b)** Test site with clayey silt soils. **(c)** Test site with gravels and sands. **(d)** Test site with patterned ground. **(e)** Waveform data from the measurements at different offsets in horizontal distance. **(f)** Experimental dispersion image for R1 wave. **(g)** Experimental dispersion image for R2 wave

3. More generally, there is a lack of references addressing issues which the authors mention. For an example, the applications (early warning systems and permafrost carbon feedback vulnerability) are frequently mentioned, but have to be more documented.

In this paper, our results demonstrate the potential of seismic surface wave testing accompanied with our proposed hybrid inverse and poromechanical dispersion model for the assessment and quantitative characterization of permafrost sites. Its applications for early detection and warning systems to monitor infrastructure impacted by permafrost-related geohazards, and to detect the presence of layers vulnerable to permafrost carbon feedback and emission of greenhouse gases into the atmosphere will be the goal of our future studies. Currently, there is no advanced physics-based monitoring system developed for the real-time interpretation of seismic measurements.

As such, active and passive seismic measurements can be collected and processed using the proposed hybrid inverse and poromechanical dispersion model for the assessment and quantitative characterization of permafrost sites at various depths in real-time. In the future study, we will focus on the development of an early warning system for the long-term tracking of permafrost conditions. The early warning system can be used to collect seismic measurements and predict the physical and mechanical properties of the foundation permafrost. The system then reports periodic variations in physical (mostly ice content) and mechanical properties of the permafrost being monitored. The same method being applied on different dates (e.g. seasonal basis) can be used to record the change of properties of the permafrost site, and then warn on the degradation of the permafrost exceeding the threshold. The value of the threshold (or critical values) will require more in-depth research to be determined. The early detection and warning systems can be beneficial in monitoring the condition of the foundation permafrost and preventing excessive thawing settlement and significant loss in strength. Similarly, we can detect the presence of peat (based on the physical and mechanical properties) which is vulnerable to permafrost carbon feedback and emission of greenhouse gases into the atmosphere. It's reported that the soils in the permafrost region hold twice as much carbon as the atmosphere does (almost 1,600 billion tonnes) (Schuur et al., 2015). The thawing permafrost can rapidly trigger landslides and erosion. Current climate models assume that permafrost thaws gradually from the surface downwards (Schuur et al., 2015). However, several meters of soil can become destabilized within a few days or weeks instead of a few centimeters of soil thawing each year (Schuur et al., 2015). The missing element of the existing studies and models is that the abrupt permafrost destabilization can occur and contribute to more carbon feedback than the existing models predict as the permafrost degrades.

Reference:

Schuur, E. A., McGuire, A. D., Schädel, C., Grosse, G., Harden, J. W., Hayes, D. J., & Vonk, J. E. (2015). Climate change and the permafrost carbon feedback. *Nature*, 520(7546), 171-179.

4. Finally, uncertainties of this new method must be addressed more quantitatively, in order to better assess its benefits and drawbacks over other methods.

Root mean square value (RMS) has been added in the manuscript to quantify the misfit between the experimental and numerical dispersion curves for both R2 and R1 waves, as shown in Figure 3.

The uncertainties due to the selection of the dispersion curve from the dispersion spectra have been considered in the revised manuscript. The dispersion curve is automatically selected initially based on the highest intensity in the dispersion spectra using MASWave software (Olafsdottir et

al., 2018). Then a 90% confidence interval (labeled as lower bound, highest intensity and upper bound, as shown in Figure 2f and 2g) is considered to study the uncertainties of the selection of dispersion curve to the inversion results. Finally, a range for each parameter (e.g., the degree of saturation of unfrozen water, porosity, shear modulus and bulk modulus) is given to quantify the uncertainty. For instance, Figure 3a shows the probabilistic distribution of the degree of saturation of unfrozen water with depth in Section 1. Our results show that the active layer has a thickness of about 1.5 m. The predicted permafrost layer (second layer) has a nearly 32% of degree of saturation of unfrozen pore water. Figure 3b shows the degree of saturation of ice with depth. The degree of saturation of ice in the permafrost layer (second layer) ranges from 67% to 79%. Figure 3c illustrates the porosity distribution with depth. The porosity is around 0.60 in the first layer (active layer), from 0.40 to 0.47 in the second layer (permafrost) and from 0.56 to 0.59 in the third layer. Figure 3d and 3e show the predicted mechanical properties of the solid skeletal frame (shear modulus and bulk modulus) in each layer. It was reported by Szymański et al. (2013) that this study site also contains a lot of coarse sandy soils, gravels as well as around 20% silty clay based on the direct sampling methods at the top 15 cm. The predicted shear modulus and bulk modulus for the solid skeletal frame in the permafrost layer (second layer) are about 13 GPa and 12.7 GPa, which are in the range for silty-clayey soils (Vanorio et al. 2003) and are also consistent with the local soil types described by Szymański et al. (2013). The predicted shear modulus and bulk modulus for the solid skeletal frame in the third layer are about 4 GPa and 10 GPa, which are in the range for clayey soils (Vanorio et al. 2003). Figure 3f and 3g show the comparison between the numerical and experimental dispersion relations for R2 and R1 waves, respectively. The numerical predictions show good agreement with the experimental dispersion curves for both R1 and R2 waves.

Reference:

Olafsdottir, E. A., Erlingsson, S., & Bessason, B. (2018). Tool for analysis of multichannel analysis of surface waves (MASW) field data and evaluation of shear wave velocity profiles of soils. *Canadian Geotechnical Journal*, 55(2), 217-233.

Vanorio, T., Prasad, M., & Nur, A. (2003). Elastic properties of dry clay mineral aggregates, suspensions and sandstones. *Geophysical Journal International*, 155(1), 319-326.

Szymański, W., Skiba, S., & Wojtuń, B. (2013). Distribution, genesis, and properties of Arctic soils: a case study from the Fuglebekken catchment, Spitsbergen. *Polish Polar Research*, 289-304.

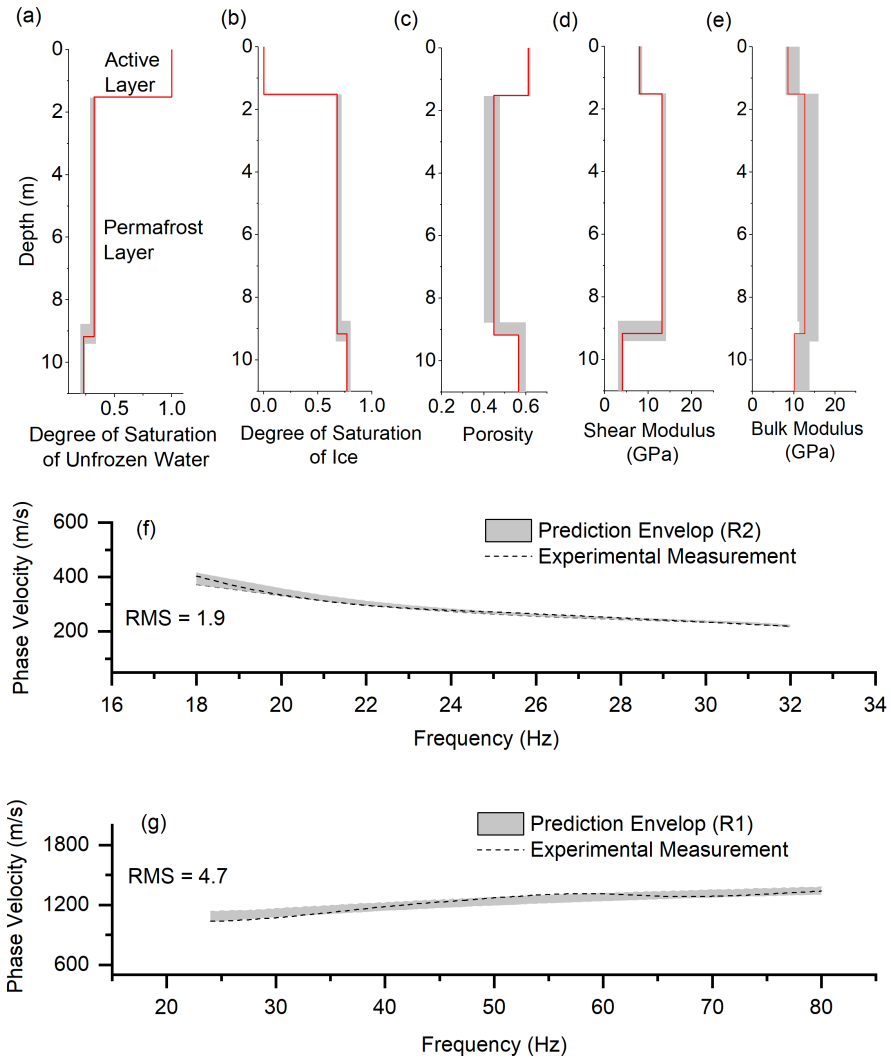


Figure 3: Surface wave inversion results for Section 1: 0m to 120m. **(a)** Degree of saturation of unfrozen water, **(b)** Degree of saturation of ice, **(c)** Porosity distribution, **(d)** Shear modulus of solid skeletal frame, **(e)** Bulk modulus of solid skeletal frame, **(f)** Experimental and numerical dispersion curves for R2 wave, **(g)** Experimental and numerical dispersion curves for R1 wave.

2 Specific comments

Applications : early warning systems and permafrost carbon feedback vulnerability: I suggest to add more details about what could be applied, and more referenced. Otherwise, these applications would be mention with caution only in the discussion part.

Its applications for early detection and warning systems to monitor infrastructure impacted by permafrost-related geohazards, and to detect the presence of layers vulnerable to permafrost carbon feedback and emission of greenhouse gases into the atmosphere are provided with more details. Active and passive seismic measurements can be collected and processed using the proposed hybrid inverse and poromechanical dispersion model for the assessment and quantitative characterization of permafrost sites at various depths. In the future study, we will focus on the development of an early warning system for the long-term tracking of permafrost conditions. The early warning system can be used to collect seismic measurements and predict the physical and mechanical properties of foundation permafrost. The system then reports a periodic variation of physical (mostly ice content) and mechanical properties of the permafrost being monitored over time. The same method being applied on different times (e.g. seasonal basis) can be used to record the change of properties of the foundation permafrost, and then warn on the level of degradation of the permafrost exceeding the threshold. The value of the threshold (or critical values) will require more in-depth research to be determined. The early detection and warning systems can be beneficial in monitoring the conditions of the foundation permafrost and preventing excessive thawing settlement and significant loss in strength. Similarly, we can detect the presence of peat (based on the physical and mechanical properties) which is vulnerable to permafrost carbon feedback and emission of greenhouse gases into the atmosphere. It's reported the soils in the permafrost region hold twice as much carbon as the atmosphere does (almost 1,600 billion tonnes) (Schuur et al., 2015). The thawing permafrost can rapidly trigger landslides and erosion. Current climate models assume that permafrost thaws gradually from the surface downwards (Schuur et al., 2015). However, several meters of soil can become destabilized within a few days or weeks instead of a few centimeters of soil thawing each year (Schuur et al., 2015). The missing element of the existing studies and models is that the abrupt permafrost destabilization can occur and contribute to more carbon feedback than the existing models predict as the permafrost foundation degrades.

Reference:

Schuur, E. A., McGuire, A. D., Schädel, C., Grosse, G., Harden, J. W., Hayes, D. J., & Vonk, J. E. (2015). Climate change and the permafrost carbon feedback. *Nature*, 520(7546), 171-179.

Discussion : In Figure 7c is shown the results of the inversion of shear modulus over the offset distance. The reader can observe a huge value of shear modulus in the permafrost layer located at a offset distance from 500m to 600m. Why this order of magnitude much higher than other parts of the whole profile ? To my mind, this results must be addressed in the discussion as well.

The higher value of shear wave velocity at the Sections 4 and 5 (spanning from 360-600 m, as shown in Figure 5) is due to the higher value of the R1 wave dispersion curve. As shown in Figure 4b, the dispersion curves of the R1 wave at Section 4 and Section 5 are relatively higher than those at the other three sections. The reason for a relatively higher R1 wave velocity in the Sections 4 and 5 could be the presence of the gravel or larger boulders, as discussed by Glazer et al., 2018

for the testing site. It was reported by Szymański et al. (2013) that this study site also contains a lot of coarse sandy soils and gravels based on the direct sampling methods at the top 15 cm. Figure 5e shows the variation of the shear modulus of soil skeleton predicted by the proposed hybrid inverse and multi-phase poro-mechanical approach. The predicted shear modulus in the first layer at the offset distance of 0 to 360 m ranges from 4 GPa to 7.9 GPa, which represents clay soils (Helgerud et al. 1999). At the offset distance from of 360 to 600 m, the estimated shear modulus in the first layer ranges from 27 GPa to 33 GPa, which corresponds to soils with calcite constituent (Helgerud et al. 1999). Calcite most commonly occurs in sedimentary rock or gravels (Schmid et al., 1987), which is consistent with the field description given by Glazer et al. 2020 and Szymański et al. (2013).

Reference:

Glazer, M., Dobiński, W., Marciniak, A., Majdański, M., & Błaszczuk, M. (2020). Spatial distribution and controls of permafrost development in non-glacial Arctic catchment over the Holocene, Fuglebekken, SW Spitsbergen. *Geomorphology*, 358, 107128.

Schmid, S. M., Panozzo, R., & Bauer, S. (1987). Simple shear experiments on calcite rocks: rheology and microfabric. *Journal of structural Geology*, 9(5-6), 747-778.

Szymański, W., Skiba, S., & Wojtuń, B. (2013). Distribution, genesis, and properties of Arctic soils: a case study from the Fuglebekken catchment, Spitsbergen. *Polish Polar Research*, 289-304.

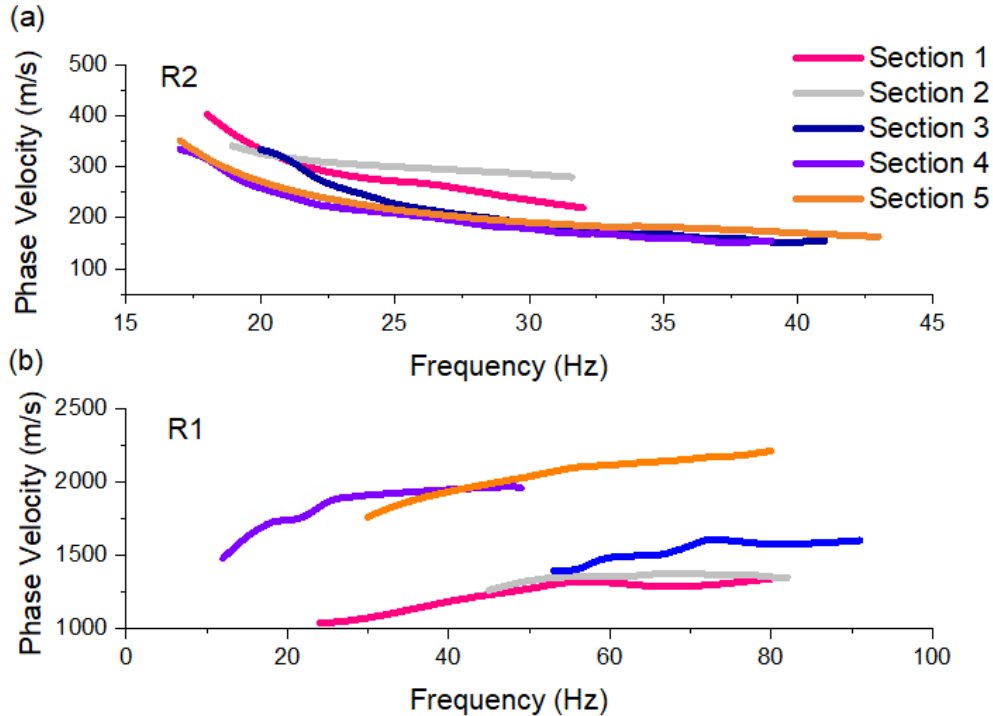


Figure 4: Summary of dispersion measurements for Section 1 to 5. (a) Dispersion curves of R2 wave. (b) Dispersion curves of R1 wave.

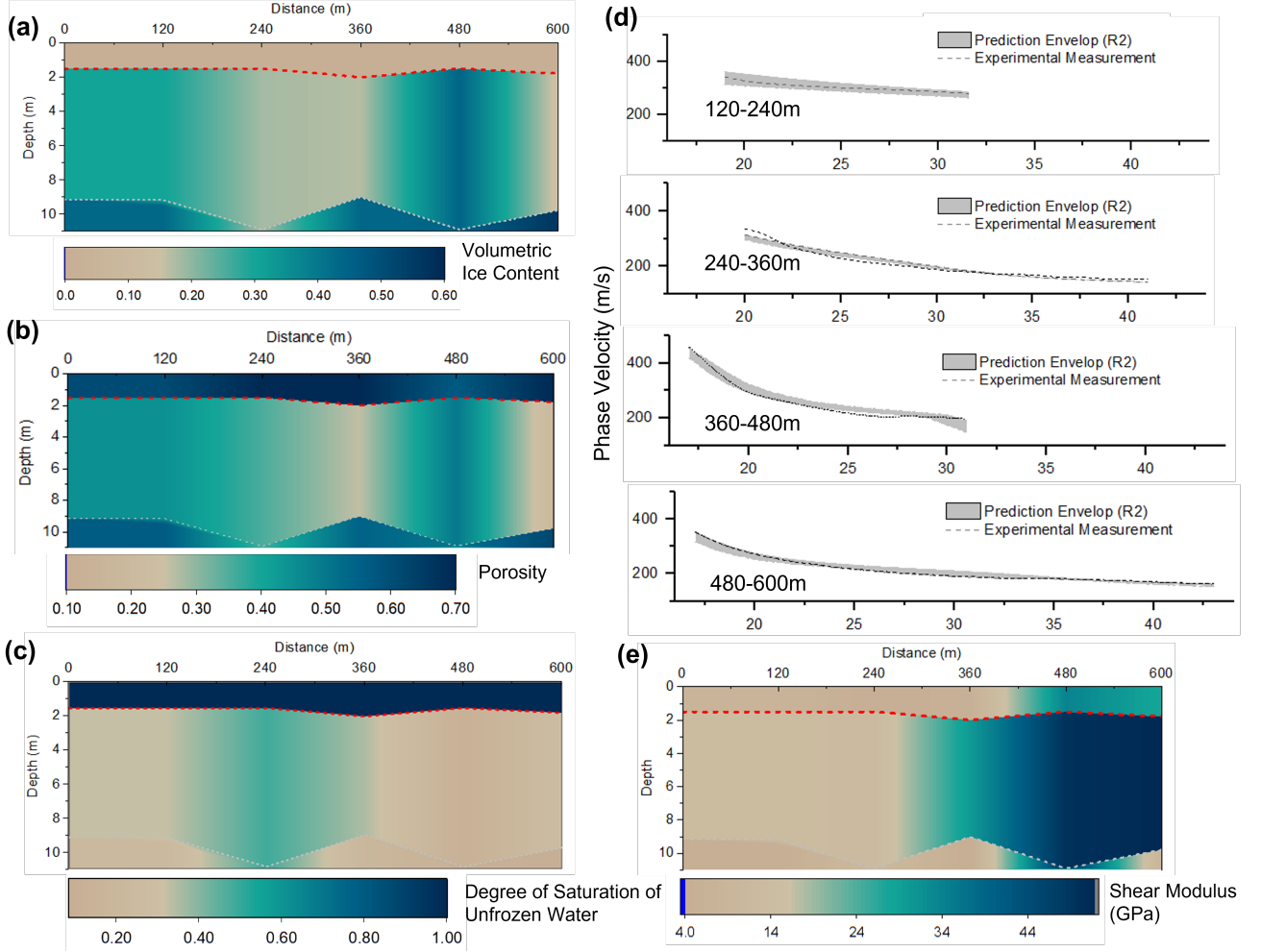


Figure 5: Summary of the inversion results at the offset distance from 0 m to 600 m. **(a)** Volumetric ice content distribution. **(b)** Soil porosity distribution. **(c)** Distribution of the degree saturation of unfrozen water. **(d)** Comparison between the numerical and experimental dispersion curves for R2 wave. **(e)** Distribution of the shear modulus of the solid skeletal frame.

L237 : according to this sentence, the ground temperature is deduced from soil temperature among others. How did you get this soil temperature data (modeled, measured on the field) ?

The ground temperature was estimated based on an empirical relation. By an empirical relation between the unfrozen water content, porosity, and soil temperature (Liu et al., 2019), we can roughly estimate the average ground temperature distribution in the test site.

The empirical relation is shown in Equation 1.

$$\theta_w = \theta_r + (\theta_{wo} - \theta_r)e^{a(T-T_0)} \quad (1)$$

where θ_r is the residual volumetric water content; a is the curve fitting parameter; T_0 is the freezing temperature considered as 0°C .

Reference:

Liu, H., Maghoul, P., & Shalaby, A. (2019). Optimum insulation design for buried utilities subject to frost action in cold regions using the Nelder-Mead algorithm. *International Journal of Heat and Mass Transfer*, 130, 613-639.

Uncertainties : RMS values have to be systematically computed, in order to quantitatively assess the accuracy of all steps of your inversion algorithm. For example, in Figure B3 : why such a misfit between R1 experimental and numerical dispersion curves, comparative to other locations ? I suggest to add a discussion of this issue.

Root mean square value (RMS) has been added in the manuscript to quantify the misfit between experimental and numerical dispersion curves for both R2 and R1 waves.

In our previous inversion analysis, we assumed that the last layer in our model is the unfrozen ground which may be unrealistic considering that the penetrating depth is roughly half of the maximum wavelength (Olafsdottir et al., 2018). For instance, the maximum wavelength in Section 1 is about 22 m (calculated using a phase velocity of 404 m/s at the frequency of 18 Hz). The maximum wavelength for Section 2 to 5 can be calculated in a similar manner. The average maximum wavelength for the entire investigation areas is around 21 m. Therefore, the penetrating depth in the MASW survey presented in this study is only about 11 m. It was reported that the permafrost layer in the studied site can go up to 100 m (Dolnicki et al., 2013; Glazer et al., 2018). Therefore, in the revised paper, we considered the last layer to have a degree of saturation of unfrozen water ranging from 1% to 99%. In this way, the last layer can be either permafrost or unfrozen ground. We have also applied the automatic methods for the selection of dispersion curves (instead of relying on visual inspection that we used in the original draft) using MASWave software (Olafsdottir, 2018). The misfits (RMS) between the R1 experimental and numerical dispersion curves at Section 4 have been significantly reduced from 49.6 to only 4.7, as shown in Figure 6g.

Reference:

Glazer, M., Dobiński, W., Marciniak, A., Majdański, M., & Błaszczuk, M. (2020). Spatial distribution and controls of permafrost development in non-glacial Arctic catchment over the Holocene, Fuglebekken, SW Spitsbergen. *Geomorphology*, 358, 107128.

Dolnicki, P., Grabiec, M., Puczko, D., Gawor, L., Budzik, T., & Klementowski, J. (2013). Variability of temperature and thickness of permafrost active layer at coastal sites of Svalbard.

Olafsdottir, E. A., Erlingsson, S., & Bessason, B. (2018). Tool for analysis of multichannel analysis of surface waves (MASW) field data and evaluation of shear wave velocity profiles of soils. *Canadian Geotechnical Journal*, 55(2), 217-233.

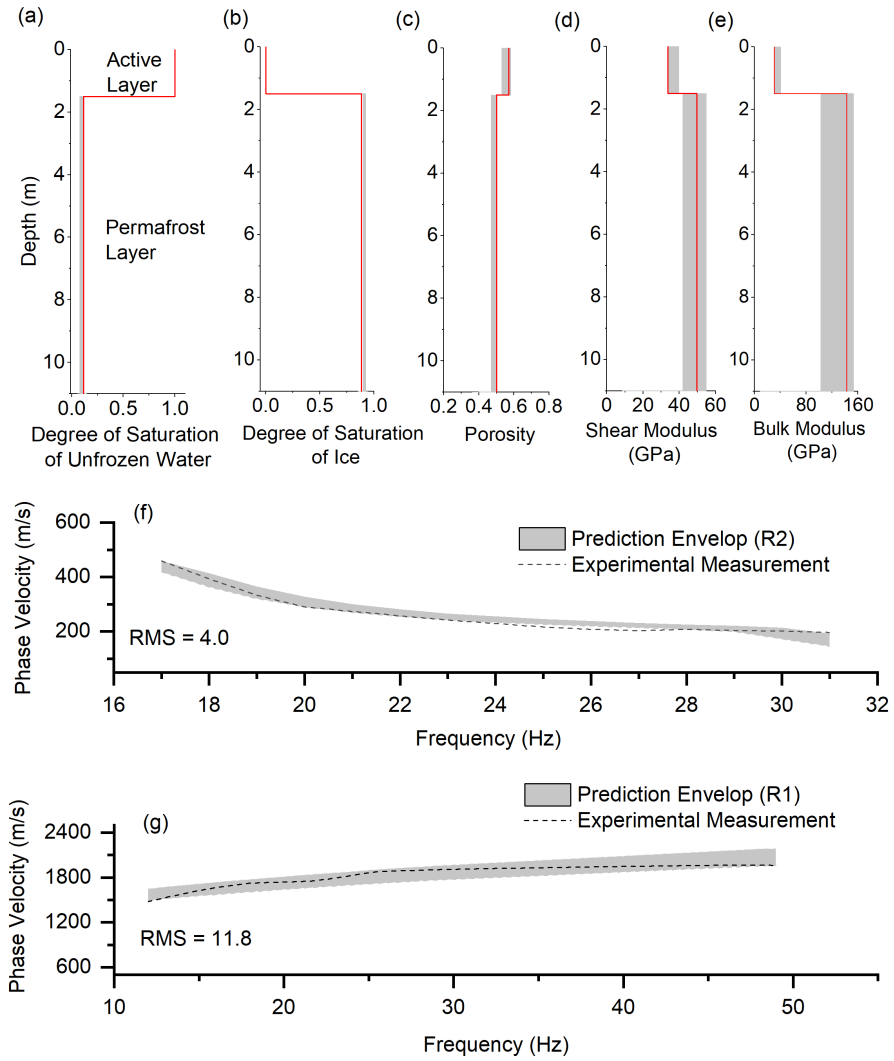


Figure 6: Surface wave inversion results for Section 4 (from 360m to 480m). **(a)** Degree of saturation of unfrozen water, **(b)** Degree of saturation of ice, **(c)** Porosity distribution, **(d)** Shear modulus of solid skeletal frame, **(e)** Bulk modulus of solid skeletal frame, **(f)** Experimental and numerical dispersion curves for R2 wave, **(g)** Experimental and numerical dispersion curves for R1 wave.

3 Technical corrections

Abstract :

L.5 : the term “relatively” is quite imprecise for an abstract, I suggest to remove it.

We have removed the term ‘relatively’.

L.7 : “Permafrost and soil layers” is inappropriate, since permafrost are considered as soil as well. Maybe replace it by “active and frozen permafrost layers” ?

We have replaced ‘permafrost and soil layers’ with ‘active and frozen permafrost layers’.

L.8 : “shear and bulk moduli”

The ‘shear modulus and bulk modulus’ are widely used in the literature. We think it is still best to keep the current form so that readers can easily follow the definition of those parameters in the three-phase poromechanical model.

Introduction:

L16 to 19 : I would add some references about permafrost thermal definition and permafrost basics.

References have been added for the permafrost definition and its basics.

Permafrost is defined as the ground that remains at or below 0°C for at least two consecutive years (Riseborough et al., 2008). The shallower layer of the ground in permafrost areas, termed as the active layer, undergoes seasonal freeze-thawing cycles (Shur et al., 2011). The thickness of the active layer depends on local geological and climate conditions such as vegetation, soil composition, air temperature, solar radiation and wind speed (Liu et al., 2019).

Reference:

Riseborough, D., Shiklomanov, N., Etzelmüller, B., Gruber, S., & Marchenko, S. (2008). Recent advances in permafrost modelling. *Permafrost and Periglacial Processes*, 19(2), 137-156.

Shur Y., Jorgenson M.T., Kanevskiy M.Z. (2011). Permafrost. In: Singh V.P., Singh P., Haritashya U.K. (eds) *Encyclopedia of Snow, Ice and Glaciers*. *Encyclopedia of Earth Sciences Series*.

Liu, H., Maghoul, P., Shalaby, A., & Bahari, A. (2019). Thermo-hydro-mechanical modeling of frost heave using the theory of poroelasticity for frost-susceptible soils in double-barrel culvert sites. *Transportation Geotechnics*, 20, 100251.

L16 : I would replace “upper” by “shallower”

Shallower layer is used in the revised manuscript.

L17 : The expression “freeze-thawing cycles” is more common, maybe replace by it.

We have revised it accordingly.

L27 : I would add at least one reference for ice wedge definition.

References to be added for the formation of ice wedge.

Ice wedges are large masses of ice formed over many centuries by repeated frost cracking and ice vein growth (Harry et al., 1988).

Reference:

Harry, D. G., & Gozdzik, J. S. (1988). Ice wedges: growth, thaw transformation, and palaeoenvironmental significance. *Journal of Quaternary Science*, 3(1), 39-55.

L28 to 37 : For these important applications that you mention, more reference and details are expected. For example, does the terms “thaw-stable” and “thaw-unstable” well documented ?

These terms have been well documented and commonly used in the literature. We have added more references.

Design and construction of structures on permafrost normally follow one of two broad principles which are based on whether the frozen foundation soil in ice-rich permafrost is thaw-stable or thaw-unstable. This distinction is determined by the ice content within the permafrost. Ice-rich permafrost contains ice in excess of its water content at saturation and is thaw unstable (Shur and Goering, 2009). The construction on thaw-unstable permafrost is challenging and requires remedial measures since upon thawing, permafrost will experience significant thaw-settlement and suffer loss of strength to values significantly lower than that for similar material in an unfrozen state. Consequently, remedial measures for excessive soil settlements or design of new infrastructure in permafrost zones affected by climate warming would require a reasonable estimation of the ice content within the permafrost (frozen soil). The rate of settlement relies on the mechanical properties of the foundation permafrost at the construction site. Furthermore, a warming climate can accelerate the microbial breakdown of organic carbon stored in permafrost and can increase the release of greenhouse gas emissions, which in return would accelerate climate change (Schuur et al., 2015).

Reference:

Shur, Y., & Goering, D. J. (2009). Climate change and foundations of buildings in permafrost regions. In *Permafrost soils* (pp. 251-260). Springer, Berlin, Heidelberg.

Schuur, E. A., McGuire, A. D., Schädel, C., Grosse, G., Harden, J. W., Hayes, D. J., & Vonk, J. E. (2015). Climate change and the permafrost carbon feedback. *Nature*, 520(7546), 171-179.

L29 : I would remove “amount of”

It has been removed.

L38 to L50 : for all the geophysical methods on permafrost, maybe more references are expected.

In this paragraph, we have included 14 references for various non-seismic geophysical methods (e.g., remote sensing, GPR, ERT).

L51 to L60 : a reference for the MASW is expected. For passive methods using ambient seismic noise on permafrost sites, you can add recent references in mountain permafrost (Guillemot 2019, Lindner 2021, Albaric 2021), to develop the state of the art about these methods.

For the MASW test on permafrost, references (Dou and Ajo-Franklin, 2014; Glazer et al., 2020) are given in the manuscript. We have also added the recommended reference in this paper (however the references for Guillemot 2019 and Lindner 2021 were not found).

Reference:

Albaric, J., Kühn, D., Ohrnberger, M., Langet, N., Harris, D., Polom, U., & Hillers, G. (2021). Seismic monitoring of permafrost in Svalbard, Arctic Norway. *Seismological Society of America*, 92(5), 2891-2904.

L61 : In this paragraph, I would add some sentences to define shortly but precisely all the four terms that you mention in your approach : “hybrid”, “inverse”, multi-phase” and “poromechanical”.

The ‘hybrid’ indicates the proposed method requires both forward solver and inverse algorithm. The forward solver is used to numerically calculate the physics-based dispersion curves for both R1 and R2 wave modes given the soil properties. The inverse solver is used to inversely (meaning of ‘inverse’) obtain the physical and mechanical properties of soils given the seismic measurements. The ‘multi-phase’ indicates the soil has three phases including solid skeleton frame, pore-water and pore-ice. The ‘poromechanical’ refers to the frame of the poroelastic model that was originally developed by Biot, 1956 and its extension for frozen soils by Leclaire et al., 1994 and Carcione et al., 2000.

Reference:

Biot, M. A. (1956). Theory of elastic waves in a fluid-saturated porous solid. 1. Low frequency range. *J. Acoust. Soc. Am.*, 28, 168-178.

Carcione, J. M., & Seriani, G. (2001). Wave simulation in frozen porous media. *Journal of Computational Physics*, 170(2), 676-695.

Leclaire, P., Cohen-Ténoudji, F., & Aguirre-Puente, J. (1994). Extension of Biot’s theory of wave propagation to frozen porous media. *The Journal of the Acoustical Society of America*, 96(6), 3753-3768.

L64-L65 : I would remove these sentence about potential applications, since you already mention them above. Maybe you can even suggest these application in the discussion and/or conclusion

parts.

It has been removed.

L70 : remove the article “the” in “for the assessment”

It has been removed.

Methods:

L74 : change “the overview” to “an overview”

It has been revised accordingly.

L75 : “surface wave measurements” Maybe you must develop the technique used in details, or precise if these seismic tests are active or passive.

These measurements can be both active and passive since the dispersion model is independent of the seismic source. In this study, the seismic measurements were collected using the active seismic source.

L100-102 : Are this statement and this equation for extracting Rayleigh wave dispersion relation ? If yes, please precise explicitly.

Yes. We have explicitly mentioned this equation is used to describe the dispersion relation of Rayleigh waves.

L103 : I would replace “a constant frequency” by “one given frequency”

It has been revised in the manuscript.

L199 : I would add “respectively” in this sentence

We have added ‘respectively’ in this sentence.

L122 : please, precise what are the two tuning parameters. Are they chosen among the optimization variables mentioned above ?

The two tuning parameters are the number of samples and the number of resampled Voronoi cells (Sambridge 1999). These two tuning parameters are different from the optimization variables (physical and mechanical properties).

Sambridge, M. (1999). Geophysical inversion with a neighbourhood algorithm—I. Searching a parameter space. *Geophysical journal international*, 138(2), 479-494.

L138 : the term “Here” is not clear, you must precise if you mind “in our model” or more focused on one layer of your model.

We have replaced 'here' with 'In this paper'.

L147 to L159 : This paragraph would be improved by adding some references or figures that illustrates your statements. Actually, it is not very clear for the readers whether the elements are your contribution, or from the current state of the art. For example : the existence of two Rayleigh waves, the respective dependency of R1 and R2 waves to parameters (mechanical and physical). If references exist about these questions, you must add them here. Overall, some physical interpretations will be appreciated : for example, is the higher R1 velocity than R2 velocity easily interpretable in a physical point of view ? Is the difference of sensitivity to physical and mechanical properties between R1 and R2 surprising or expectable ? Why ?

The existence of two Rayleigh waves and the respective dependency of R1 and R2 waves to parameters (physical and mechanical properties) are also the contribution from this research.

To physically interpret the two Rayleigh waves, a uniform frozen soil layer is used to show the propagation of different types of P and S waves and subsequently the formation of Rayleigh waves (R1 and R2) at the surface. It is assumed that an impulse load with a dominant frequency of 100 Hz is applied at the ground surface. The wave propagation analysis was performed in clayey soils by assuming a porosity (n) of 0.5, a degree of saturation of unfrozen water (S_r) of 50%, a bulk modulus (K) of 20.9 GPa and a shear modulus (G) of 6.85 GPa for the solid skeletal frame (helgerud et al., 1999). The velocities of the P1 and P2 waves are calculated as 2,628 m/s and 910 m/s, respectively, based on the relations given in Appendix A in the manuscript. Similarly, the velocities of the S1 and S2 waves are calculated as 1,217 m/s and 481 m/s, respectively. We also found the velocity of R1 and R2 is 1,150 m/s and 450 m/s using the three-phase dispersion relation derived in this paper (Equation 1). It is known that the Rayleigh wave is slightly slower than the shear wave velocity and the ratio of the Rayleigh wave and shear wave velocity ranges from 0.92-0.95 for Poisson's ratio greater than 0.3 (Kazemirad et al., 2013). From this analysis, we found the ratio of R1 and S1 wave velocity is around 0.93. Similarly, the ratio of R2 and S2 wave velocity is around 0.94. Therefore, we can conclude that R1 waves appear due to the interaction of P1 and S1 waves since the phase velocity of R1 waves is slightly slower than the phase velocity of S1 waves. Similarly, R2 waves appear due to the interaction of P2 and S2 waves since the phase velocity of R2 waves is also slightly slower than the phase velocity of S2 waves. This explains why R1 velocity is higher than R2 velocity.

The P1 and S1 waves are strongly related to the longitudinal and transverse waves propagating in the solid skeletal frame, respectively, but are also dependent on the interactions with pore ice and pore water (Carcione and Seriani, 2001). We have proved that R1 waves appear due to the interaction of P1 and S1 waves (see the previous graph). Therefore, the phase velocity of the R1 wave is dependent on both mechanical properties and physical properties. The P2 and S2 waves propagate mainly within pore ice (Leclaire et al., 1994). Hence, the phase velocity of the R2 wave is almost independent of the mechanical properties of the solid skeletal frame, while it is strongly affected by the porosity and degree of saturation of ice.

Reference:

Carcione, J. M., & Seriani, G. (2001). Wave simulation in frozen porous media. *Journal of Computational Physics*, 170(2), 676-695.

Leclaire, P., Cohen-Ténoudji, F., & Aguirre-Puente, J. (1994). Extension of Biot's theory of wave propagation to frozen porous media. *The Journal of the Acoustical Society of America*, 96(6), 3753-3768.

Kazemirad, S., & Mongeau, L. (2013). Rayleigh wave propagation method for the characterization of a thin layer of biomaterials. *The Journal of the Acoustical Society of America*, 133(6), 4332-4342.

Helgerud, M. B., Dvorkin, J., Nur, A., Sakai, A., & Collett, T. (1999). Elastic-wave velocity in marine sediments with gas hydrates: Effective medium modeling. *Geophysical Research Letters*, 26(13), 2021-2024.

L174 : if you can, precise the type of geophones (type, natural frequency)

The information for geophones has been given in the revised manuscript. The MASW test was performed by using 60 geophone receivers with a frequency of 4.5 Hz spaced at regular 2 m intervals.

L181 : why "almost completely frozen" ? Precise why you choose the value 85% for the degree of saturation of unfrozen water.

In the revised manuscript to address your comment, we have considered that the degree of saturation of unfrozen water in the active layer is 100% since the test site was extremely wet during the MASW test and the ERT results reported by Glazer et al. (2020) proved that the active layer is most likely completely unfrozen during the MASW testing performed in September. For the permafrost layer (second layer), we have considered that the degree of saturation of unfrozen water is between 1%-85% to be conservative. The degree of saturation of unfrozen water in the third layer is between 1%-100% (permafrost or unfrozen ground, which is to be determined).

L195 : I would add a reference for illustrating this statement

A reference has been added for this sentence: 'However, the mechanical properties of permafrost reveal the mineral composition of the soil and soil type (Helgerud et al., 1999), which is valuable in the classification of ice-rich permafrost or even detection of whether the permafrost layer is prone to greenhouse gases carbon dioxide and methane emission to the atmosphere'.

Reference:

Helgerud, M. B., Dvorkin, J., Nur, A., Sakai, A., & Collett, T. (1999). Elastic-wave velocity in marine sediments with gas hydrates: Effective medium modeling. *Geophysical Research Letters*, 26(13), 2021-2024.

L210 : the term "sufficiently close" must be completed by a quantitative assessment (RMS ?).

RMS value has been added in the revised manuscript to quantify the misfits between numerical and experimental dispersion curves: The numerical predictions show good agreement with the experimental dispersion curves for both R1 (RMS value of 1.9) and R2 (RMS value of 4.7) waves.

L227 : “We also predicted”

We have added ‘We also predicted’ in the manuscript.

L239 : I suggest to replace “is highly related” by “could highly related”

It has been replaced with ‘could highly relate’.

Discussion and conclusions:

L249 : “makes the analysis more efficient” : you must tell more about this statement : What do you compare this method to ? And, have you done a quantitative assessment to support this discussion?

In this paper, we proposed a separate inversion instead of a joint inversion methods. We firstly used the dispersion of R2 waves to characterize the physical properties of the layers. After obtaining the physical properties. Then the mechanical properties can be derived based on the dispersion relation of the R1 wave mode in a similar manner. The proposed approach (inversion based on R2 and R1 wave modes) in this paper simplifies the inversion of the multi-layered three-phase poromechanical model since the dependent optimization variables are largely reduced. Therefore, the statement of “makes the analysis more efficient” is compared with the case where inversion analysis is performed to determine both physical and mechanical properties at the same time.

L255 to 257 : this sentence must be documented by at least one reference.

A reference has been added for this sentence.

Reference:

Hodgkins, S. B., Tfaily, M. M., McCalley, C. K., Logan, T. A., Crill, P. M., Saleska, S. R., & Chanton, J. P. (2014). Changes in peat chemistry associated with permafrost thaw increase greenhouse gas production. *Proceedings of the National Academy of Sciences*, 111(16), 5819-5824.

L276 : for the case of a potential early warning system, how do you plan to deal with the seasonal variations (ex: freeze-thawing cycles of the active layer) that you would measure over one year? Do you have any idea how to model and remove such environmental influences that are not related to damage? And how to fix critical values ? If you have any ideas on this issues, you would be welcome to mention them, in order to strengthen your discussion on this potential application.

The applications of our proposed method for early detection and warning systems to monitor infrastructure impacted by permafrost-related geohazards are provided with more details. Active and passive seismic measurements can be collected and processed using the proposed hybrid inverse and poromechanical dispersion model for the assessment and quantitative characterization of permafrost sites at various depths. In the future study, we will focus on the development of an early warning system for the long-term tracking of permafrost conditions. The early warning system can be used to collect seismic measurements and predict the physical and mechanical properties of foundation permafrost in real-time. The system then reports periodic variations of physical (mostly ice content) and mechanical properties of the permafrost being monitored. The same method being applied on different times (e.g. seasonal basis) can be used to record the change of properties of the permafrost site, and then warn on the level of degradation of the permafrost exceeding the threshold. The value of the threshold (or critical values) will require more in-depth research to be determined. The early detection and warning systems can be beneficial in monitoring the state of the foundation permafrost and preventing excessive thawing settlement and significant loss in strength. Similarly, we can detect the presence of peat (based on the physical and mechanical properties) which is vulnerable to permafrost carbon feedback and emission of greenhouse gases into the atmosphere. It's reported the soils in the permafrost region hold twice

as much carbon as the atmosphere does (almost 1,600 billion tonnes) (Schuur et al., 2015). The thawing permafrost can rapidly trigger landslides and erosion. Current climate models assume that permafrost thaws gradually from the surface downwards (Schuur et al., 2015). However, several meters of soil can become destabilized within a few days or weeks instead of a few centimeters of soil thawing each year (Schuur et al., 2015). The missing element of the existing studies and models is that the abrupt permafrost destabilization can occur and contribute to more carbon feedback than the existing models predict as the permafrost foundation collapses.

Reference:

Schuur, E. A., McGuire, A. D., Schädel, C., Grosse, G., Harden, J. W., Hayes, D. J., & Vonk, J. E. (2015). Climate change and the permafrost carbon feedback. *Nature*, 520(7546), 171-179.

Figures:

Figure 1: I would precise in the legend that variable (n , S_r , H , K , G) are defined for each layer (layer 1, layer 2, layer 3).

We have defined variables for each layer with a subscript ranging from 1 to 3 to represent layer 1 to layer 3.

Figure 2 : this figure is not very explicit. Please clarify the definition of G , m , h .

We have moved this figure to Appendix. The term G (the stiffness matrix of a layer) has been defined in Equation C21. The h parameter represents the number of layer with finite thickness. The m parameter represents the half-space layer.

Figure 3 : colorbar ?

Colorbar has been added in the revised manuscript.

Figure 4 : a map with geographic location of the study site in Svalbard, and another focusing on the location of all different profiles of geophones that we used for this study would be appreciated.

A map with geographic location of the study site in Svalbard has been added in the manuscript. The location of different profiles of geophones in the testing site is also added in the manuscript.

Figure 5-6 : the vertical-horizontal ratio scaling to modify in graphs ?

It would be much more appreciated if reviewer can clarify how the scaling should be done.

Figure 7 : You show results of some outputs of your inversion, but what about the results of bulk modulus ? For (d), scaling has to be modified. And also for the sake of simplicity, the predicted average soil temperature distribution may be removed from this figure, since this variable do not seem to be useful for the study.

The bulk modulus is found not as sensitive as the shear wave velocity, which is confirmed from our previous publications (Liu et al., 2020). This can also be seen in the inversion results shown in Figure 3e where the bulk modulus has relatively larger uncertainties. Therefore, we did not show the contour plot for the bulk modulus. In the revised manuscript, we also removed the inversion results for the estimation of soil temperature.

Reference:

Liu, H., Maghoul, P., Shalaby, A., Bahari, A., & Moradi, F. (2020). Integrated approach for the MASW dispersion analysis using the spectral element technique and trust region reflective method. *Computers and Geotechnics*, 125, 103689.

Appendices:

Appendices A, C and D: there is a lack of references in these parts. I suggest to add at least Carcione & Seriani (2001) and Leclaire (1994).

References (Carcione & Seriani (2001) and Leclaire (1994)) have been added.

Reference:

Carcione, J. M., & Seriani, G. (2001). Wave simulation in frozen porous media. *Journal of Computational Physics*, 170(2), 676-695.

Leclaire, P., Cohen-Ténoudji, F., & Aguirre-Puente, J. (1994). Extension of Biot's theory of wave propagation to frozen porous media. *The Journal of the Acoustical Society of America*, 96(6), 3753-3768.

Appendix B : in all figures you show both saturation degree of unfrozen water and saturation degree of ice, but only one seems to be useful, since the two variables are directly linked together. Furthermore, what about the results of the layer thickness from this surface wave inversion? It could be appropriate to show them as well. Again, for R1 and R2 experimental and numerical dispersion curves, it should be good to precise misfits through RMS values.

Even though the degree of saturation of unfrozen water is directly related to the degree of saturation of ice, we still think it might be helpful to include both of them. The plot of the degree of saturation of unfrozen water can directly show readers the characteristic of the active layer; whereas the degree of saturation of ice can directly show readers the characteristic of permafrost layers. Also, the thickness is given in the vertical axis. We also added the RMS values for the comparison between the experimental and numerical dispersion curves for both R1 and R2 waves.

L297 : I suggest to add "respectively"

We have added 'respectively' in this sentence.

L382 : "Convention" instead of "convection"

It has been corrected in the revised manuscript.

L396 : "The values of each component" instead of "The value of each components"

It has been corrected in the revised manuscript.

Appendix D : L432 : I suggest to remove "the matrix formed by" for consistency

It has been removed in the revised manuscript.

Appendix A: Definition of Phase Velocities

The velocities of the three types of P waves are determined by a third degree characteristic equation (Leclaire et al., 1994 and Carcione et al., 2000):

$$\Lambda^3 \tilde{R} - \Lambda^2 \left((\rho_{11} \tilde{R}_{iw} + \rho_{22} \tilde{R}_{si} + \rho_{33} \tilde{R}_{sw}) - 2(R_{11} R_{33} \rho_{23} + R_{33} R_{12} \rho_{12}) \right) + \Lambda \left((R_{11} \tilde{\rho}_{iw} + R_{22} \tilde{\rho}_{si} + R_{33} \tilde{\rho}_{sw}) - 2(\rho_{11} \rho_{23} R_{23} + \rho_{33} \rho_{12} R_{12}) \right) - \tilde{\rho} = 0$$

where

$$\begin{aligned} \tilde{R} &= R_{11} R_{22} R_{33} - R_{23}^2 R_{11} - R_{12}^2 R_{33} \\ \tilde{R}_{sw} &= R_{11} R_{22} - R_{12}^2 \\ \tilde{R}_{iw} &= R_{22} R_{33} - R_{23}^2 \\ \tilde{R}_{si} &= R_{11} R_{33} \\ \tilde{\rho} &= \rho_{11} \rho_{22} \rho_{33} - \rho_{23}^2 \rho_{11} - \rho_{12}^2 \rho_{33} \\ \tilde{\rho}_{sw} &= \rho_{11} \rho_{22} - \rho_{12}^2 \\ \tilde{\rho}_{iw} &= \rho_{22} \rho_{33} - \rho_{23}^2 \\ \tilde{\rho}_{si} &= \rho_{11} \rho_{33} \end{aligned}$$

The roots of the third degree characteristic equation, denoted as Λ_1 , Λ_2 and Λ_3 , can be found by computing the eigenvalues of the companion matrix (Horn and Johnson, 2012). The velocities of the three types of P-wave ($v_{p1} > v_{p2} > v_{p3}$) are given as follows:

$$v_{p1} = \sqrt{\frac{1}{\Lambda_1}}; \quad v_{p2} = \sqrt{\frac{1}{\Lambda_2}}; \quad v_{p3} = \sqrt{\frac{1}{\Lambda_3}}$$

The velocities of the two types of S-wave are determined by a second degree characteristic equation:

$$\delta^2 \rho_{22} \tilde{\mu}_{si} - \delta(\mu_{11} \tilde{\rho}_{iw} + \mu_{33} \tilde{\rho}_{sw}) + \tilde{\rho} = 0$$

The roots of this second degree characteristic equation is denoted by δ_1 and δ_2 . The velocities of the two types of S-wave ($v_{s1} > v_{s2}$) are given as follows:

$$v_{s1} = \sqrt{\frac{1}{\delta_1}}; \quad v_{s2} = \sqrt{\frac{1}{\delta_2}}$$